International Journal of Biological Macromolecules 85 (2016) 82–91

Contents lists available at ScienceDirect

International Journal of Biological Macromolecules

journal homepage: www.elsevier.com/locate/ijbiomac

Radiation-synthesized protein-based drug carriers: Size-controlled BSA nanoparticles

R.G. Queiroz[a,*], G.H.C. Varca[a,*], S. Kadlubowski[b], P. Ulanski[b], A.B. Lugão[a]

[a] Instituto de Pesquisas Energéticas e Nucleares (IPEN/CNEN-SP), Av. Prof. Lineu Prestes, 2242, Cidade Universitária, 05508-000 São Paulo, SP, Brazil
[b] Institute of Applied Radiation Chemistry, Lodz University of Technology, Wroblewskiego 15, 93-590, Lodz, Poland

ARTICLE INFO

Article history:
Received 9 November 2015
Received in revised form
18 December 2015
Accepted 21 December 2015
Available online 28 December 2015

Keywords:
Bovine serum albumin
Gamma-irradiation
Protein-based nanoparticles
Protein crosslinking
Nanocarrier

ABSTRACT

Nanotechnology has broadened the options for the delivery of agents of biotechnological and clinical relevance. Currently, attention has been driven towards the development of protein-based nanocarriers due to high the biocompatibility and site-specific delivery. In this work we report radiation-synthesized bovine serum albumin nanoparticles as an attempt to overcome limitations of available albumin particles, as a novel route for the development of crosslinked protein nanocarriers for the administration of chemotherapic agents or radiopharmaceuticals. Albumin containing phosphate buffer solutions were irradiated using γ-irradiation at distinct cosolvent concentrations—ethanol or methanol. Nanoparticle size was followed by DLS and bityrosine crosslinking formation using fluorescence measurements and SDS-PAGE. In addition, computational experiments were performed to elucidate the mechanism and pathways for the nanoparticle formation. The synthesis of BSA nanoparticles using γ-irradiation in the presence of a cosolvent allowed the formation of the nanoparticles from 7 to 70 nm without the use of any chemical crosslinker as confirmed by SDS-PAGE and DLS analysis. The combination of cosolvent and γ-irradiation allowed a fine tuning with regard to protein size.

1. Introduction

Albumin is a globular protein that abounds in human plasma and egg [1]. Its monomeric structure comprises around 600 amino acids with a total molecular weight of 66 kDa. Albumin plays an important role in the organism, e.g.: as an oncotic agent, scavenger of free radicals, transporting agent for a wide range of metabolites and drugs. It also participates in coagulation pathways with basically an anticoagulant effect and in the maintenance of the osmotic pressure [2].

There are different types of albumin, known as ovalbumin, bovine serum albumin (BSA) and human serum albumin (HSA). The last ones have a few similarities regarding size, molecular weight (MW) and structure. For example, BSA has MW of 66.500 kDa and 585 amino acids and HSA 69.323 kDa with 609 residues [1,3]. Up to now, its properties, functions and applications were extensively investigated and a wide range of applications and uses in the pharmaceutical and biotechnological field emerged. For instance, the use of albumin as a model protein for studies on novel proteins or delivery systems is widely used and accepted all around the globe and the main focus on its uses in the pharmaceutical field is due to the high biocompatibility of these proteins with the human body, with no pronounced side effects or allergenic reactions [1,3].

Regarding albumin ability to bind to many kinds of drugs, many efforts have been made in order to develop or produce medicines that associated with albumin could have their bioavailability enhanced. Additionally, the use of an albumin-based nanoparticle as a drug carrier confers other additional advantages over conventional release systems, such as improved interaction of the drug with bio-interfaces, better uptake in inflamed and tumor tissue, half-life and biocompatibility, negligible immunogenicity and toxicity, controlled release and so on [4,5].

For the past three decades the technology of using micro and nanoparticles for drug delivery has brought to light new perspectives regarding the administration of several types of pharmaceutics [1,6–8]. From a size perspective, nanoparticles offer better properties when compared to microparticles due to the highlighted chemical, physical and biological properties. As an example, nanoparticles (NP) may be easily removed from the liver and spleen

* Corresponding authors.
E-mail addresses: rodgqueiroz@gmail.com (R.G. Queiroz), varca@usp.br (G.H.C. Varca).

http://dx.doi.org/10.1016/j.ijbiomac.2015.12.074
0141-8130/

Table 1
Particle sizes of non-irradiated and 10 kGy irradiated BSA at different solvent concentrations.

Solvent concentration (% v/v)	Particle size (mean ± SD in d nm) Non-irradiated		Irradiated[a]	
	EtOH	MeOH	EtOH	MeOH
0	6.6 ± 0.3	6.6 ± 0.3	16.6 ± 2.3	16.6 ± 2.3
10	9.0 ± 0.4	–	10.0 ± 0.6	–
20	12.0 ± 1.1	9.4 ± 0.6	12.8 ± 2.8	10.3 ± 1.1
30	14.3 ± 1.3	9.0 ± 1.7	25.1 ± 2.9	10.2 ± 1.5
35	15.8 ± 2.1	–	60.2 ± 6.0	–
40	20.7 ± 2.0	10.6 ± 2.3	68.7 ± 6.4	15.7 ± 2.4
45	–	13.6 ± 3.2	–	20.4 ± 4.5
50	–	20.9 ± 6.0	–	48.2 ± 6.3

[a] γ-irradiation of BSA (20 mg mL^{-1}) was performed at a dose rate (determined by alanine dosimetry) of 1.031 kGy h^{-1} and totally absorbed dose of 10 kGy.

leading to a shorter time retention in the body if compared to submicron [9].

The use of biomolecules to develop nanoparticles is widely studied and protein-based nanoparticles are biopolymers that have demonstrated to be a promising alternative for a new generation of drug delivery systems, in particular for chemoterapeuticals and cancer treatments in general [8]. In the case of albumin-based nanoparticles, whether for diagnostics, imaging or drug-delivery, many efforts are being made to encapsulate chemotherapic and oncotic agents into this drug delivery system [5,6]. The motivation behind the use of albumin for chemotherapeutics is based on the premise that most of chemotherapics are difficult to be administered via parenteral or intravenous application, which requires the use of additional chemical agents, like Chremophor EL, a solubilizing system used on taxanes formulation. Based on this idea the first commercially available nanocarrier for this family, named as CApxol^{TM}, was developed using paclitaxel formulated with albumin in order to improve the bioavailability of the drug and remove the other chemical agents, known to potentially induce side effects and undesirable reactions [10].

The continuous search for alternative systems for the administration of taxanes led to the approval by FDA of another medicine, known as Abraxane®, a formulation based on albumin-bound paclitaxel nanoparticles synthesized by the so-called nab^{TM} (nanometer albumin bound) technology [11]. This new kind of drug has been evaluated in clinical trials for several types of cancer and the results obtained showed an enhancement of the nab-paclitaxel towards the formulation done with Chremophor EL [11].

Regarding to the synthesis of albumin nanoparticles, one important issue that not only improves the efficacy of the system from a bioavailability point of view, but also stands as a challenge to be overcome by the available methods is the size control [12,13]. On this account, many synthesis routes were studied in order to control the size of the particles. Besides the nab-paclitaxel technology, there are other ways to synthesize albumin nanoparticles, e.g., desolvation, emulsification, spray drying and self-assembly [1]. The desolvation technique in particular has been improved and demonstrated good reproducibility in obtain narrow particle sizes distribution. This method is based on the use of a solvent to promote the protein aggregation and an additional crosslinking agent (e.g., glutharaldehyde) to avoid a redissolvation of the particles when solubilized or redispersed in water [13].

Soto-Espinoza et al. [14] demonstrated the possibility to use radiation to achieve albumin nanoparticles by the use of acetonitrile and/or other solvents, which could potentially confer additional advantages if compared to albumin itself with regard to drug release purposes. At a later stage Varca et al. [15,16] advanced the discussion towards the development of protein-based nanoparticles by applying γ-irradiation to papain solutions, a model enzyme widely used in industry, considering solvent and protein concentration, and different conditions of synthesis including the influence of irradiation dose.

The goal of this research was to deliver detailed information about the radiation synthesis of BSA nanoparticles, a technique capable of producing crosslinked BSA nanoparticles of controllable particle size by the combination of protein desolvation

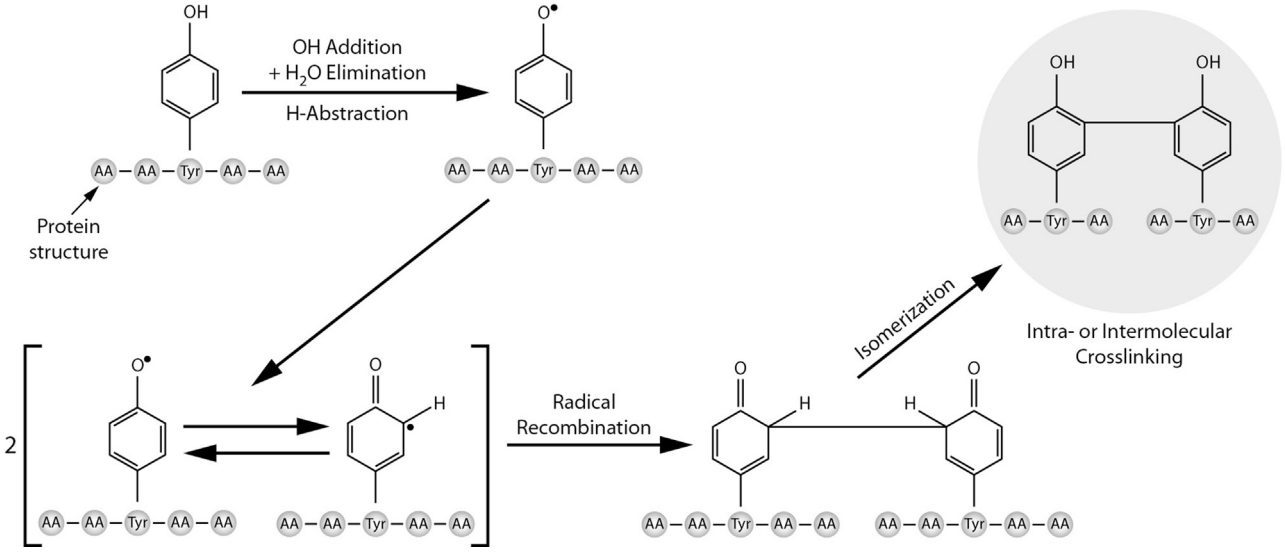

Fig. 1. Mechanism of bityrosine crosslinking in proteins by γ-irradiation. Adapted from Giulivi et al. [29].

followed by crosslinking using γ-irradiation. For such purpose the effects of irradiation in different media over BSA particle size and bityrosine crosslinking formation have been carefully monitored using dynamic light scattering, fluorescence measurements and SDS-PAGE. Additional computational experiments were performed to elucidate the mechanism and pathways for the nanoparticle formation. The technique does not require the use of monomers or chemical crosslinkers, and therefore, the produced protein-based nanoparticle comprise less toxic and novel option of protein- based drug carrier for the administration of drugs such as chemotherapeuticals, radiopharmaceuticals or other drugs of interest.

2. Experimental

2.1. Materials

Bovine Serum Albumin (BSA, Heat shock fraction, purity ≥98%), Bis-acrylamide, Tris, β-mercaptoethanol, glycerine, Coomassie Blue G250 were purchased from Sigma–Aldrich® (USA). Molecular weight marker Spectra Multicolor High Range Protein Ladder was purchased from Thermo Scientific™ (USA). Ethanol (EtOH), methanol (MeOH), anhydrous di- and monobasic phosphate, and acetic acid were acquired from Synth® (Brazil). All reagents were of analytical grade.

2.2. Procedures

2.2.1. Synthesis of albumin nanoparticles by γ-irradiation

BSA was dissolved in phosphate buffer (PB) 50 mM at pH 7.2 to reach concentration of 100 mg mL^{-1}. Aliquots of 1 mL of the BSA solution were transferred to glass vials containing PB followed by slow addition of cosolvent to reach 10–40% EtOH or 20–50% MeOH (v/v) concentrations and BSA concentration of 20 mg mL^{-1} in a final volume of 5 mL. The whole procedure was performed on ice bath and after preparation the flasks were hermetically sealed. The samples were allowed to stabilize overnight and then exposed to γ-irradiation in a mini-cooler with synthetic ice packs, at the dose of 10 kGy and dose rate of 1.03 $kGyh^{-1}$, as determined by alanine dosimetry [17], using ^{60}Co as radioactive source in Gammacell 220 irradiator (Atomic Energy of Canada Limited, Ottawa, Canada). The samples were stored at ±4 °C prior to analysis. Controls were prepared under the same conditions.

2.2.2. Particle size characterization

Particle size measurements were performed by Dynamic Light Scattering (DLS) analysis on a Zetasizer Nano ZS90 (Malvern Instruments GmbH, Germany) device at 20 °C and 90° scattering angle. The samples were filtered using 0.45 μm cellulose acetate syringe filters prior to analysis. Results were reported by average hydrodynamic diameter by number using 3 sets of 3 runs for each measurement.

2.2.3. SDS-PAGE

Aliquots of BSA and BSA nanoparticles were diluted in distilled water and added to 10 μL of loading buffer with β-mercaptoethanol as a reducing agent to reach protein concentration of 2 μg/μl. The samples were rapidly vortexed and heated up to 70 °C for 5 min. Aliquots of 10 μL of the samples and protein markers were loaded on a 7.5% polyacrylamide gel (Bis–Tris) with a 4% stacking gel. The SDS-PAGE was performed on an SE250 Mighty Small II Mini Vertical Electrophoresis Unit (Hoefer Inc., USA) at constant voltage of 90 V. After fixation, the proteins were stained with coomassie blue. The procedure was performed according to Laemmli [18].

2.2.4. Protein crosslinking

The samples were diluted using PB to reach equivalent absorbance of approximately 0.25 at λ = 280 nm. The samples were then checked for bityrosine emission using λ_{Ex} = 325 nm λ_{Em} = 350–600 nm, at a scan speed of 240 nm/min on a Spectramax i3 (Molecular Devices, USA). The procedure was performed according to Varca et al.]16] and Dimarco et al. [19] and the spectra was normalized by considering the maximum values registered for native BSA solution as a reference value of 1.

2.2.5. Structural approach

Solvent accessible surface area was calculated using the program Volume, Area, Dihedral Angle Reporter -VADAR [20]. Van der Waals radii was selected from Shrake and Rupley [21], and all hydrogen bonds were set to water. Graphical representation was performed using Jmol v. 12.0.4.1 [22]. All calculations were performed with files available at the Protein Data Base (PDB)—(4FS5.pdb -2.47 Å resolution).

3. Results and discussion

3.1. BSA nanoparticles synthesis by γ-irradiation

BSA nanoparticles were synthesized by combining the effects of solvent (desolvation), in order to promote a microenvironment suitable for the nanoparticle formation, and exposure to γ-irradiation, applied for the crosslinking of the nanoparticles. Protein crosslinking brings about modifications that may modulate catalytic activities of enzymes, provide markers recognition, induce selective digestion among others [20,23].

3.1.1. Effect of solvent concentration

The so called DLS, also known as photon correlation spectroscopy stands as a technique suitable for the detection of nanoparticle size of a wide variety of compounds in solution, which allows a proper monitoring of molecular changes in a submicron- to nanoscale perspective. In our studied systems, the DLS results showed a slight but gradual increase over BSA particle size, ranging from 6.6 ± 0.3 nm (in diameter) for native BSA in absence of cosolvent up to about 20.7 ± 2.0 nm in presence of 40% EtOH (v/v) (Table 1). Above 40% EtOH concentrations the solution presented huge white aggregates and a phase separation and as a consequence the DLS analysis was inappropriate. The same behavior occurred for non-irradiated BSA in presence of MeOH. Whatsoever the size increase in this case was lower ranging from 6.6 ± 0.3 nm to 10.6 ± 2.3 nm in solutions containing up to 40% (v/v) MeOH. Above 45%, particle size increased up to 20.9 ± 6.0 nm reaching the same size as observed for albumin at 40% EtOH (Table 1).

The irradiated solutions containing BSA in the absence of cosolvents had a size increase when compared with the non-irradiated solutions, while the latter presented a particle size of 6.6 ± 0.3 nm, the former was 16.6 ± 2.3 (Table 1). The combination of both cosolvent and γ-irradiation allowed the synthesis of protein nanoparticles in controlled matter with respect to the particle size.

In a more detailed approach, the nanoparticles synthesized in presence of EtOH presented size ranging from 10.0 ± 0.6 nm to 68.7 ± 6.4 nm. Meanwhile, for the nanoparticles synthesized in presence of MeOH, the size range was from 10.3 ± 1.13 nm to 48.2 ± 6.3 nm.

In terms of possible combined effects between solvent concentration and the changes in the ionic strength of the medium preliminary results indicated that concerning the molarity variation of the solvent in the assayed samples, calculated as around 50 mM for native BSA down to 25 mM at 50% cosolvent concentration, held no effect over particle size. The strong aggregation

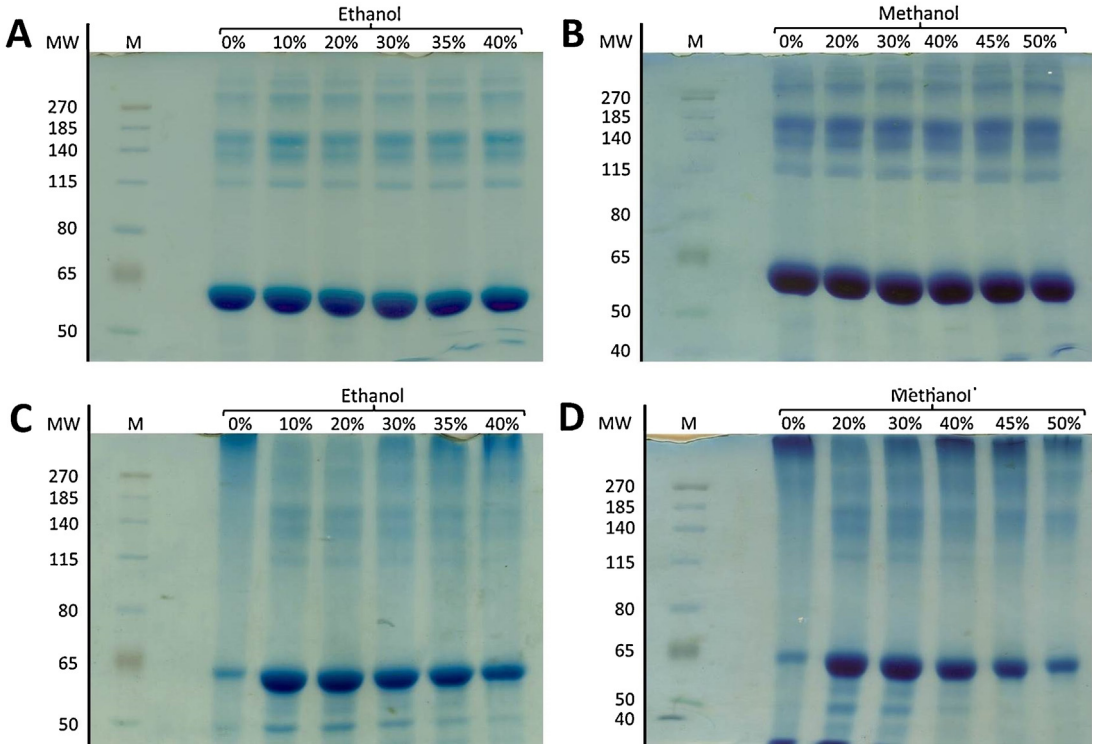

Fig. 2. SDS-PAGE with 7.5% polyacrylamide gel using reducing sample buffer containing native BSA at distinct (A) EtOH and (B) MeOH concentrations, and γ-irradiated BSA at distinct ethanol (C) and (D) methanol concentrations. *MW: Molecular weight and M: Standard molecular weight marker.

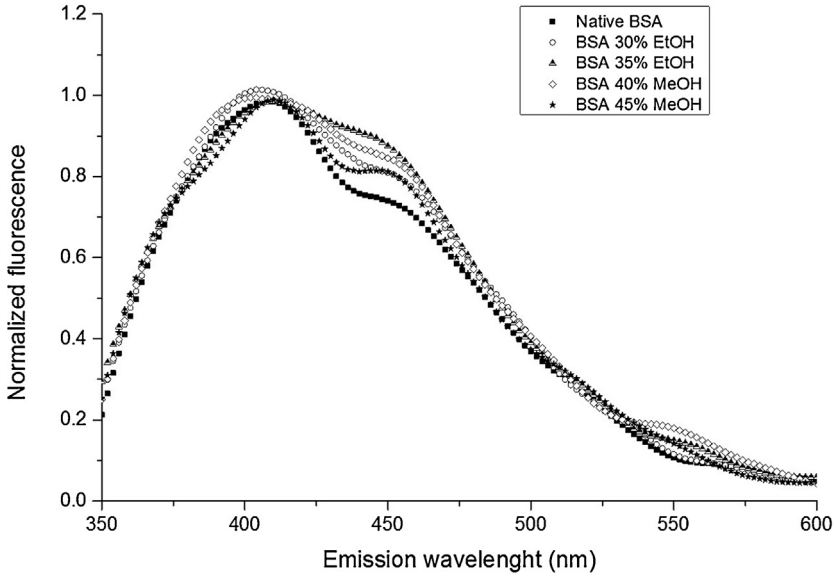

Fig. 3. Evaluation of bityrosine spectra of native and the non-irradiated BSA solutions at distinct ethanol and methanol concentrations.

properties induced by the desolvating agent, mainly at high concentrations, were also expected to take over any effect resultant from changes in ionic strength.

In a comparison between the BSA nanoparticles of BSA of the same concentrations in EtOH and MeOH (20%, 30% and 40%), the BSA nanoparticles synthesized in the presence of MeOH were smaller than the ones synthesized in presence of EtOH, and changes were more gradual as a function of concentration. This information suggested that MeOH induced less pronounced changes as a function of concentration, under the given conditions, if compared to EtOH. MeOH was also capable of modifying the BSA in a more controllable way if compared to EtOH. The advantage and motivation behind the use of a desolvating agent, MeOH or EtOH, was related to the possibility to solubilize very hydrophobic or poorly soluble drugs more efficiently than in water, especially during drug loading process onto the nanoparticles.

Upon irradiation the BSA solutions at higher EtOH concentrations showed an abrupt increase by means of particle size from the 30% EtOH solution to the 35% EtOH. BSA solutions containing more than 40% (v/v) EtOH led to the formation of insoluble macro-aggregates which made the solutions inadequate for DLS measurements and therefore such results are not reported in the

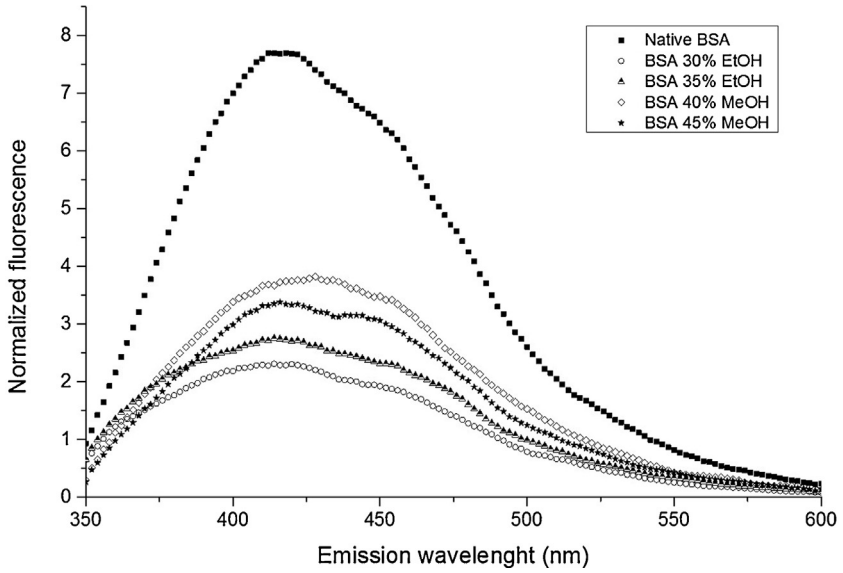

Fig. 4. Evaluation of bityrosine spectra of (10 kGy) γ-irradiated native and BSA solutions at distinct ethanol and methanol concentrations.

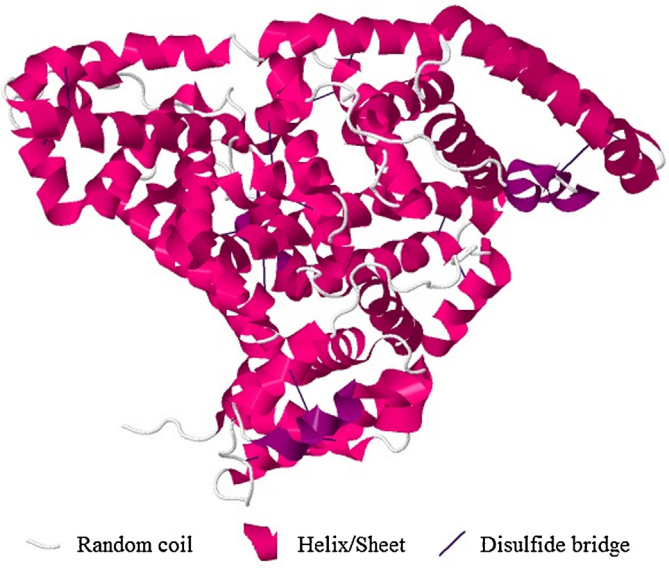

Fig. 5. Crystal structure of Bovine Serum Albumin (Protein data bank code 4F5S).

text. At 50% MeOH concentrations, the BSA solution turned into a viscous, gel-like solution. This is an indicative that at higher solvent concentrations, the induced microenvironmental changes were capable of dramatically altering protein conformation, leading to the formation of macro-aggregates and larger particles rather than submicron or nano-aggregates. In practical terms, the agglomeration effect was too strong as the solution became more viscous and to opaque due to the high ethanol content.

Also, BSA nanoparticles obtained using 30%, 35% and 40% EtOH concentrations were about 3 times higher than the particles obtained in MeOH. It is important to observe that the results of BSA nanoparticles in presence of EtOH loses its control size manner when its particle size shifted from 25.05 nm at 30% to 60.15 nm at 35% EtOH, revealing an abrupt increase. Overall BSA nanoparticle synthesized in MeOH did not increase as much in presence of EtOH, followed by gradual increase proportional to solvent concentration, again reinforcing that a more controllable process of synthesis was achieved in presence of MeOH.

According to literature [24] the main difference between the effect of each solvent is related to its polarity, in such a way that as protein desolvation takes place the solvation layer around the protein decreased as the organic solvent, MeOH and EtOH in our case, progressively displaced water from the protein surface to the hydration layers around the solvent molecules. As a result of the smaller hydration layers protein aggregations begins to take place trough field proximity forces, such as electrostatic and dipole–dipole, in other words the difference of each solvent is related to its capacity to displace the water molecules from protein.

In conclusion, concerning the behaviour of BSA towards the effects of solvents by means of DLS, both EtOH and MeOH were capable of inducing protein particle size increase andin agreement with the literature, the more solvent applied the larger the aggregates [24]. Yoshikawa et al. [25] reported that the increase of EtOH concentrations in solution of bovine albumin resulted in a decrease of its solubility. Regarding MeOH, the same behaviour was observed in our experiments, suggesting that the same type of mechanism could be happening, although higher MeOH concentrations were required to reach the similar particle sizes.

The purpose of applying γ-radiation to the samples was related to the possibility to provide a similar effect of glutharaldehyde, a commonly used cross-linking agent applied in desolvation processes [13] in order to stabilize the formed protein structure. The selection of 10 kGy as a standards dose for the synthesis was based on previous works which identified this dose as optimum for protein crosslinking by γ-irradiation [14,16].

Highlighted advantages of the high energy irradiation are related to the absence of monomers or toxic compounds and the possibility to combine nanoparticle formation and in situ sterilization simultaneously [26] inside the final package and with no or minor influence of temperature.

At this point, the question that arises is whether these size-increase effects were reversible or not, concerning the effects of the desolvation agent alone and irradiation combined or not with desolvating agent, and also if such changes were a result of the size of a single/crosslinked particle or an aggregate of crosslinked particles. Although these topics remain as subject for further studies, the lack of crosslinking in absence of irradiation, as described further on this article (see Section 3.2.2), indicated that in accordance to the mechanism proposed, such the changes caused by the desolvating agent were rather physical than chemical and thus not permanent.

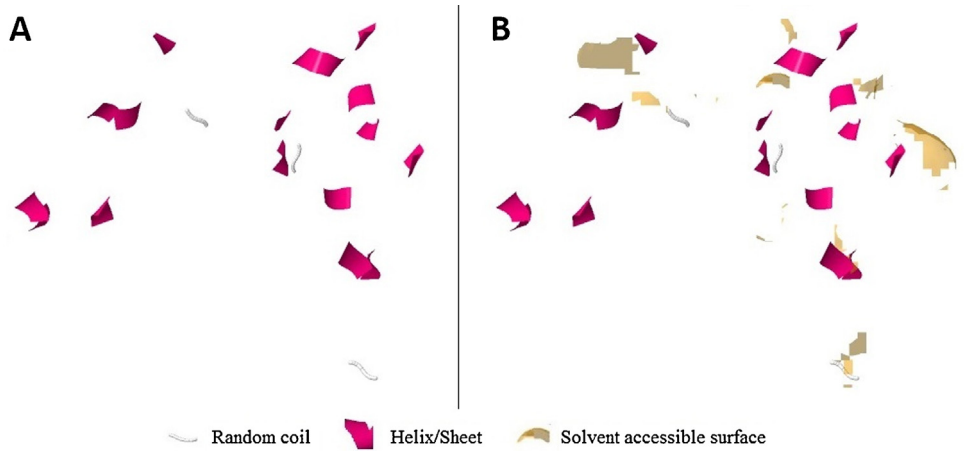

Fig. 6. BSA tyrosine radicals (A) and their solvent accessibility (B) (Protein data bank code 4F5S). *Solvent accessible surface-shadow.

The irradiation of BSA in absence of cosolvent led to particles diameter of about 16.6 nm. Although this shift is limited if compared to the use of solvents, in which according to our results may lead to BSA nanoparticles of about 68.7 nm as observed for EtOH, this suggested that the radiation may be also explored to promote the synthesis of protein nanoparticles without the use of solvents. The use of cosolvents, on the other hand, allowed a size controllable synthesis as a function of cosolvent concentrations. The dose dependence as well as the influence of other parameters such as dose rate, presence of oxygen over the protein crosslinking in the proposed system remain as a subject for further studies.

3.2. Mechanism of BSA nanoparticle formation by γ-irradiation

The effect of high energy irradiation such as electron-beam or γ-irradiation over proteins in aqueous solutions has been widely studied, including the effects over BSA [27,28]. Depending upon the presence of gases, the main product of such exposure is the formation of bityrosines [20,29]. The representative scheme of the mechanism of bityrosine formation during protein crosslinking by γ-irradiation is described in Fig. 1.

In practical terms, the oxidizing species, e.g., hydroxyl radical (•OH) formed as a result of water radiolysis, leads to protein crosslinking mainly via tyrosine radicals, Tyr-Tyr. Additional linkages include the cysteine bonding Cys–Cys, via novel disulfide bridges [28] as an example. The nature of such linkages plays a key role in the particle formation, taking into account that intramolecular crosslinks do not lead to molecular weight increase, whereas an increase in these property characterizes intermolecular binding [30].

3.2.1. Inter vs. intramolecular crosslinking

The relevance in providing a molecular weight evaluation would help clarify and contribute to a better understanding of the relationship between the nature of such linkages and the particle size increase. Particularly, the SDS-PAGE of the irradiated BSA (Fig. 2) showed a difference between irradiated solutions over the non-irradiated ones. In Fig. 2(A) the classic pattern for BSA was noted in the first column, standing as the positive control (i.e., native BSA), composed by non-irradiated solution of BSA in PB in absence of cosolvent.

All other columns, at 10%, 20%, 30%, 35% and 40% (v/v) EtOH concentrations showed the same native BSA pattern, and demonstrated that the addition of the cosolvent did not promote a crosslinking of intermolecular nature, hence indicating that the increase of the particle size revealed by DLS occurred indeed as a result of physical linkages. On the other hand, Fig. 2(C) shows a different behavior for the irradiated solutions, where in the first column, the BSA solution irradiated in the absence of cosolvent presented a strong stained band observed above 270 kDa, thus indicating protein crosslinking. Distinct authors also reported the presence of higher molecular weight bands for crosslinked HSA nanoparticles [31,32] synthesized by chemical routes.

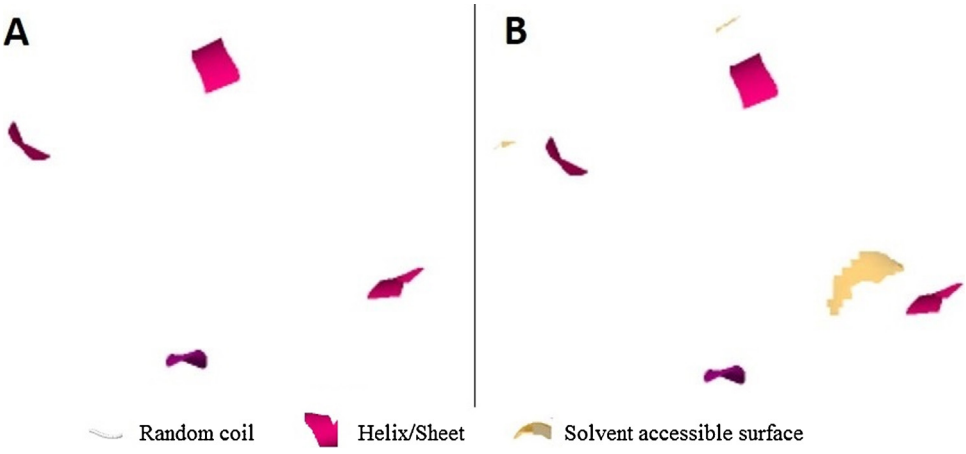

Fig. 7. BSA Methionine radicals (A) and their solvent accessibility (B) (Protein data bank code 4F5S).

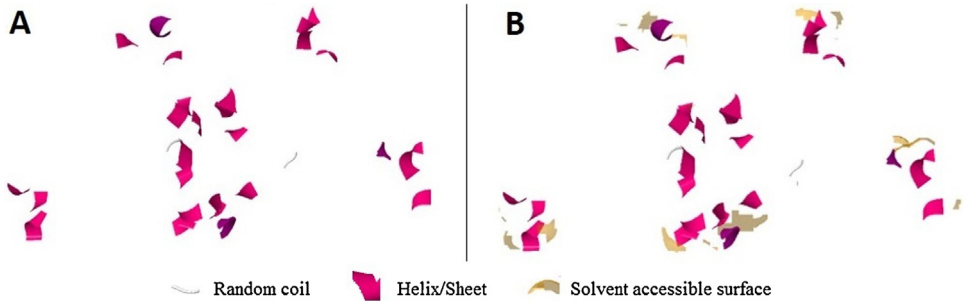

Fig. 8. BSA Cysteine radicals (A) and their solvent accessibility (B) (4F5S.pdb—2.47 Å resolution).

Overall a very strong cross-linking effect was observed in PB, a mild effect in 10% EtOH and then a gradually stronger effect with increasing EtOH concentration. The irradiated solutions in presence of EtOH showed a reduction of the main stained band of native albumin in a concentration dependant way meanwhile formation of stained aggregates with high MW (>270 kDa) were observed. At the concentrations of 10% and 20% of EtOH (v/v) there was no macro-aggregates formation, they only started to appear at the fourth column that corresponds to the solution with 30% (v/v) of EtOH. The reducing sample buffer used did not turn back the aggregates to a native albumin profile.

The use of MeOH (Fig. 2B and D) revealed the behavior profile as observed for EtOH in both gels (non-irradiated and irradiated). The formation of nanoparticles in MeOH also started at 30% (v/v) and the increase of high MW stained aggregates were gradual too. While the concentration of native albumin stain decreased along with the concentration of MeOH, the stained BSA nanoparticles (aggregates) increased. A difference was noted when the stained aggregates showed to be more concentrated in MeOH than with EtOH due to the darkest blue stain at high MW values (>270 kDa).

Irradiation of albumin solutions in absence of cosolvent also led to the NP formation as evidenced by the stains of protein aggregates that appeared above the highest MW of the marker (270 kDa). Such bands were observed in presence of both cosolvent as well. Another observation that can be spotted is the difference that appeared at low MW bands below native albumin stained band, related to the products of degradation, disappeared from the gel from 40% to 50% MeOH (v/v) while the same bands in EtOH SDS-PAGE remained.

Despite the results of size increase by DLS analysis, the SDS-PAGE experiments revealed that the aggregation promoted by the cosolvents was not responsible for the formation of nanoparticles, as observed by the bands around 66 kDa, and thus indicating a distinct mechanism of particle formation. In this particular case all concentrations of both solvents showed the same profile as for native BSA (Fig. 2A and C). On the other hand, the SDS-PAGE of the irradiated BSA presented a distinct behavior, as revealed by the bands observed above 270 kDa. This supports the crosslinking promoted by γ-irradiation. Furthermore, the stained bands on the gels at 30% or higher cosolvent concentrations revealed the same profile that was observed on SDS-PAGE of nanoHSA obtained by desolvation methods [31,32]. This molecular weight increase demonstrates experimentally a formation of crosslinks of intermolecular nature in the nanoparticle formation.

As mentioned above the minimum concentration required to induce some aggregation on the SDS-PAGE corresponded to 30% (v/v) for both cosolvents, even though the high Mw stained aggregate formed in presence of MeOH was not as intense as the one using EtOH, corroborating the DLS analysis results. At the highest concentrations, 40% EtOH and 50% MeOH the nanoparticles were formed but the solution presented physical alterations at macroscopic level, whereas the solution with EtOH showed a mass of insoluble aggregate and a formation of two phases, MeOH on the other hand presented a gel aspect. A hypothesis that can support this behaviour is related to the influence of high cosolvent and protein concentration applied in the system.

It is relevant to observe that such experiments were carried out in reducing conditions, by the use of β-mercaptoethanol and as a consequence, all cysteine linkages were reduced/broken. The high MW bands appeared in the gel after treatment and suggested that cysteine linkages did not play a major/important role in the BSA nanoparticle formation whatsoever.

3.2.2. BSA crosslinking by γ-irradiation—intermolecular bityrosine formation

The bityrosine crosslinking is by far the most common linkage observed in distinct kinds of protein–protein crosslinking, although many pathways may lead to such formation [19,29,32–35]. An experimental evaluation of the bityrosine may be assessed trough fluorescence analysis [19]. and is of key relevance when it comes to protein crosslinking. On this account BSA nanoparticles were synthesized at the selected optimum solvent concentrations of 30% and 35% EtOH and, 40% and 45% MeOH (v/v), based on particle size and SDS-PAGE, and assessed for the protein crosslinking formation by means of bityrosine according to the parameters described by several researchers [16,19,29,33].

The effect of cosolvent – EtOH or MeOH – over BSA without irradiation by means of bityrosine, is negligible as revealed in Fig. 3. Considering that no significant changes are observed and such minimum shift is more likely to be related to the changes in the microenvironment surrounding the protein and its amino acids

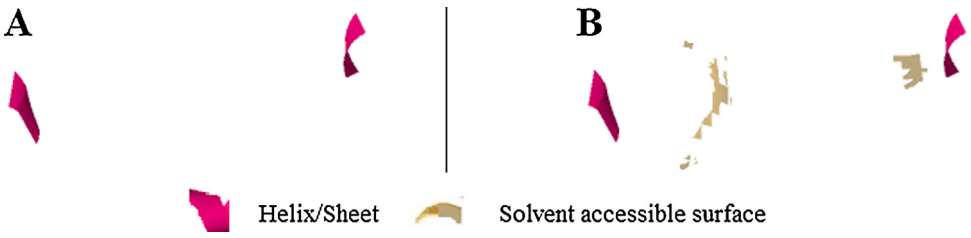

Fig. 9. BSA Tryptophan radicals (A) and their solvent accessibility (B) (4F5S.pdb—2.47 Å resolution).

rather than an increase in protein crosslinking. This information is particularly interesting, considering it also indicates that the effects promoted by the desolvation are rather physical than chemical, and thus size changes are not permanent to an extent, as described in literature [24]. The signal for bityrosine in native albumin is minimum (>200 Fluorescence Units) and normalization was required to allow a better visualization of such effect.

γ-irradiation at 10 kGy in absence of cosolvent (Fig. 4) revealed an intense increase in the bityrosine linkages of approximately 8-fold, indicating high levels of crosslinking. In presence of cosolvent γ-irradiation led to a minor signal increase if compared to irradiation alone of approximately 2- and 2.5-fold in presence of 30 and 35% EtOH and 3- and 4-fold using 35 and 40% MeOH concentrations, respectively.

BSA irradiated in presence of MeOH presented a higher intensity when compared to the samples containing the selected EtOH concentrations, highlighting the distinct behavior promoted by each cosolvent. In both cases the cosolvent was capable of inducing controlled formation of bityrosine.

In summary the results confirmed that the use of γ-irradiation led to the formation of bityrosine crosslinks in BSA in PB and with the addition of both cosolvents. The signal presented for the BSA in absence of cosolvent was higher than the samples containing EtOH or MeOH. This shift was expected considering the well established scavenger properties of both cosolvents [36,37], which in practice, decrease the amount of radicals available to interact with the protein. Corroborating these results, Varca et al. [16] reported the formation of bityrosine in papain nanoparticles synthesized by γ-irradiation and also demonstrated a major role of such linkages in the nanoparticle formation.

Although a relation between particle size and bityrosine levels may be identified as BSA with higher particle sizes presented higher bityrosines intensity, such relation could not be identified when comparing the profiles of BSA in presence of solvents, where a higher particle size was achieved with a lower bityrosine intensity if compared to BSA irradiated in PB.

Although intermolecular bityrosine linkages have been identified and extensively studied for the free radical modifications of proteins [29,34,35], other mechanisms that might be involved in the nanoparticle formation are mainly attributed to the build-up of novel disulfide bridges. The intermolecular Cys–Cys bonding is originated in a similar way of other sulfur-centered radicals via effect of the •OH over free cysteine residues thus leading to the formation of thyil radicals, that upon certain conditions, may bind to another thiol to form disulfide radical anion and then build up a disulfide bridge [34]. Whatsoever, after treatment with β-mercaptoethanol, the crosslinks were still present and indicated that the size and high molecular weight compounds were still preserved after rupture of such linkages. Rombouts et al. [38] reported that such changes mainly take place at alkaline pH. Moreover, the *in silico* approach, as explained further in this article, reveals that BSA presents only one free cysteine, revealing that this mechanism less likely to occur if compared to the Tyr as an example.

In addition to this, recent literature reports the development of HSA nanoparticles via disulfide bridges [32], and provide more detailed literature about the role of such intermolecular linkages [38]. All of them require reduction of the disulfide bridges by the use of heat or chemical treatments, also helping to support the minor role of novel Cys–Cys linkages when it comes to radiation synthesis of BSA nanoparticles.

3.2.3. BSA crosslinking by γ-irradiation—additional pathways

The free radical modification on proteins is known to be directed towards the formation of bityrosines or cysteine linkages of intermolecular nature [33,34]. The bityrosine formation may occur by distinct pathways, whether via oxidation of cysteine (Cys), methionine (Met), tryptophan(Trp), or oxidation of tyrosine (Tyr) directly, or through the attack of e^-_{aq} over disulfide bridges [33,34,39].

Particularly the rate constants of OH and e^-_{aq} reaction with BSA, around neutral pH, were established with a magnitude of about $3 \times 10^{10}\ dm^3 mol^{-1}\ s^{-1}$ [28], whereas the BSA-e^-_{aq} adduct was established at $7 \times 10^9\ dm^3 mol^{-1}\ s^{-1}$ in previous studies [40], indicating that from a radiation chemistry perspective, reactions involving the latter radical are likely to occur with a lower magnitude than reactions mediated by •OH.

In solution, the main targets by radiation are the solvent molecules. In the case of water, the •OH (highly oxidizing) and e^-_{aq} (strong reducing agent) are the most relevant free radicals formed, while in the case of alcohols, the reaction of irradiation leads to the formation of alcohol derived radicals, which are most likely to be reductive species [37]. Such radicals will then attack aromatic amino acids present in protein, phenylalanine, Trp and Tyr, as well as sulphur-centered residues, such as cysteine and methionine, depending on their oxidative or reducing properties [34]. The principle involved in each pathway varies according to the amino acid. On this account, an in silico structural approach is fundamental to provide evidences of which pathways might be more pronounced in the case of BSA nanoparticles formation by irradiation.

On a structural based approach native BSA (Fig. 5) presents 35Cys, 4 Met,20 Tyr and 2 Trp. The graphical representation corresponds to the crystal structure of BSA available at the Protein Data Base obtained, based on x-ray diffraction experiments at 2.47 Å resolution [41].

The tyrosine mediated pathway is related to one- or two-electron oxidation achieved by the reaction of oxidizing species [34,35]. As revealed by Fig. 6, BSA presents 20 Tyr residues. A few of those are solvent accessible or partially accessible, and thus prone to attack by •OH, such as Tyr-262, Tyr-400, Tyr-451 and 496 with 71, 94.5, 41.1 and 42.6 A^2 of solvent accessibility respectively. All other Tyr hold low accessibility values $\leq$33.1 A^2. This information confirms that BSA molecule presents some structural implications in terms of allowing the formation of the nanoparticles is via direct attack to Tyr, but a few residues are likely to be directly attacked from an accessibility perspective.

On the other hand, the Met pathway with regard to bityrosine formation is known to occur via direct attack by •OH which is followed by a quick intramolecular electron transfer from a neighbouring Tyr, which then leads to tyrosyl radical formation and subsequent dimerization [34,35,42]. As revealed in Fig. 7, BSA presents 4 Met residues of those only Met 547 is solvent accessible, with ASA of 63.4 A^2, and thus prone to attack by •OH or other oxidant species. The other Met residues, 87, 184 and 445, presented very low accessibility of 1.6, 16.3 and 12.3 A^2 respectively.

The case of cysteine is very unique. A majority of Cys residues present in native BSA are directly involved in the disulphide bridges that compose protein structure. As consequence all of them present very low accessibility values ranging from 0 to 39 $Å^2$. Only Cys 34 is a free cysteine. Cysteine amino acids present in BSA were represented in Fig. 8.

The cysteine mediated pathway for bityrosine remains very likely to take place. The reason behind this is based on the fact that although BSA holds only one free cysteine, the cysteine pathway may also occur as a result of reduction of the disulfide bridges which naturally occur in BSA molecule [34]. In this particular case the e^-_{aq} is responsible for such process and considering the high constant rate of the reaction between the hydrated electron and BSA, and the high amount of disulfide bridges present in the protein structure (17), this pathway also stands a possible route for the bityrosine formation.

In specific terms the e^-_{aq} attacks the disulfide bridges by H-abstraction and which them transfer the attack to a neighbouring

Tyr, to form a tyrosyl radical and then leading to the bityrosine formation [34]. A similar attack caused by alcooxyl radicals are also very likely to take place.

Taking into account the developed system any reactions of hydrated electron with BSA were expected to be of a minor rate, considering that the e^-_{aq} would be scavenged by oxygen before it can reach BSA and under such conditions, considering the reaction rate constant between oxygen and BSA with e^-_{aq} one can estimate that only 28% of the electron present in the system would react with the protein. Whatsoever, we estimated that for the samples in absence of gas purge all oxygen present in the sealed vial would be consumed as the dose reached 1 kGy.

Overall, the structural evaluation of Cys displacement along BSA molecule revealed unfavourable conditions for novel intermolecular Cys–Cys bonding, as revealed by the low accessibility values and the very low number of free residues (Fig. 8) and thus, concerning radiation processing, were very unlikely to take place. This composed a proof of the minor or negligible role of cysteine binding in the process as a result of •OH attack, indicating that this mechanism does not seem to be involved to a major extend in the nanoparticle formation. The effect of the e^-_{aq} on the other hand remains very likely to occur in addition to the alcooxyl radicals formed during EtOH or MeOH radiolysis.

The case of Trp mediated pathway is related to the one-electron transfer reaction from tyrosine to tryptophan that arises from the reaction of •OH with Trp, and then leading to the formation of the tyrosyl radical [39]. Although BSA molecule only presents 2 Trp (Fig. 9), 134 and 213 with 14.1 and 37.6 A^2 respectively, the close proximity between the Trp and Tyrosines in BSA molecule make such pathway a possible route, considering that intramolecular electron transfer may take advantage of the proximity.

In conclusion, from a structural perspective there are plenty of pathways for the formation of bityrosine crosslinking in BSA molecule during irradiation as revealed by the in silico approach. Perhaps the most relevant pathways seem to be related to the direct attack to Tyr (Tyr 262, Tyr400, Tyr451 and Tyr 496), methionine (Met 547), including Trp (Trp 213) and Cys (Cys 34) to a minor extent. The attack by the e^-_{aq} to the disulfide bridges remain as very relevant and possible pathway.

4. Conclusion

The synthesis of BSA nanoparticles using γ-irradiation in the presence of a cosolvent allowed the formation of the nanoparticles without the use of any chemical crosslinker, as confirmed by SDS-PAGE and DLS analysis. Comparing the DLS analysis, a slight increase in particle size of the non-irradiated samples, the SDS-PAGE showed that the stained proteins were different from the irradiated ones. EtOH and MeOH were capable of inducing the formation of nanoparticles with different behaviour. In a more specific way, the use of EtOH combined with irradiation led to the formation of BSA nanoparticles at EtOH concentrations ranging from 30% to 40%. In this particular case, EtOH concentrations of 30% and 35% (v/v) were more suitable for further experiments due to the size of the particles and SDS-PAGE revealed high concentration of protein aggregates with high molecular weights (>270 kDa) at these solvent concentrations. At higher EtOH concentrations, 40% and 50% (v/v), BSA presented a white coloured massive insoluble aggregate formation, suggesting that the structure of the native protein was affected and such extreme conditions, consequently, lead to the formation of an aggregate of macromolecular level. MeOH also promoted the formation of BSA aggregates although higher concentrations of this solvent were required to obtain BSA nanoparticles with considerable smaller particle size if compared to the use of EtOH. Optimized results were established as 40% or 45% MeOH. At higher concentrations (50%, v/v) a gel-like colloidal solution was observed.

γ-irradiation was effective to promote the BSA crosslinking, at the dose of 10 kGy, as revealed by the bityrosine formation monitored by fluorescence spectroscopy. The nature of such crosslinks were of intermolecular nature, as revealed by the molecular weight increase from 66 kDa (native BSA) to >270 kDa for the BSA nanoparticle observed as result of the process. This corroborates and experimentally supports the mechanisms attributed to the papain nanoparticles synthesized by γ-irradiation in previous studies.

As above mentioned, It is relevant to highlight that BSA nanoparticles were also achieved in absence of cosolvent, which suggested that some control could also be achieved only by irradiating BSA in water or buffer at different doses. Whatsoever, the synthesis of the nanoparticles, achievable by the use of the cosolvent allowed the formation of higher particle size in controllable way directly related to the cosolvent and its concentration.

The mechanism of nanoparticle formation was demonstrated by bityrosine monitoring using fluorescence spectra and confirmed by high MW bands observed on the SDS-PAGE. The bityrosine profiles indicated that irradiation in absence of cosolvents was capable of increasing considerably the bityrosine intensity, whereas as EtOH or MeOH concentration increased, a control over such formation was observed thus corroborating the size changes observed by DLS and providing an experimental evidence of the control over the nanoparticle formation. In addition, to some extent, the involvement of novel cysteine linkages in the nanoparticle formation is less likely to take place, as demonstrated by the in silico approach which revealed structural implications for the formation of the intermolecular Cys–Cys and the high molecular weight bands observed after treatment with β-mercaptoethanol in the SDS-PAGE.

Although the process takes place as results of a very complex system the computational approach on the structural properties of BSA indicated that the main pathways are related to direct attack to Tyr, or attack mediated by Met. To a minor extent, Cys and Trp pathways are also possible to take place. The attack by the e^-_{aq} to the disulfide bridges also were found to be of high relevance to the process. Whatsoever additional radiation chemistry experiments may also be required in order to clarify the exact pathway as well as the radicals that trigger nanoparticle formation.

The procedure for synthesizing BSA nanoparticles in presence of cosolvents crosslinked by γ-irradiation was successful and the cosolvent concentration played fundamental role in the process considering their ability to control the formation of BSA nanoparticles by means of particle size. We emphasize that such technique offer new advantages over conventional methods including, but not restricted to the lack of monomers in the process as well as the possibility to combine protein crosslinking (nanoparticle formation) and sterilization simultaneously inside the final package. Particularly the absence of crosslinkers in designing protein based nanostructures assures a very low residual toxicity and reduces possible productions stages related to the removal of the remaining monomers. The combination of solvent and γ-irradiation allowed a fine tuning with regard to protein size. Final applications of the technology concern the development of novel options for the administration of chemotherapeutic agents or radiopharmaceuticals, with potential therapeutic applications.

Acknowledgments

The authors would like to thank Laboratório de Biofísica (IF-USP, São Paulo, Brazil), Centro de Biotecnologia (IPEN/CNEN-SP), Fundação de Amparo a Pesquisa do estado de São Paulo (FAPESP Project number 2015/13979-0), Conselho Nacional de Desenvolvimento Científico e Tecnológico (CNPq project number

402887/2013-1) and the Nuclear and Atomic Energy Agency (CRP code F22064)—IAEA for financial support.

References

[1] A.O. Elzoghby, W.M. Samy, N.A. Elgindy, Albumin-based nanoparticles as potential controlled release drug delivery systems, J. Control. Release 157 (2012) 168–182.
[2] N. Soni, M. Margarson, Albumin. Where are we now? Curr. Anaesth. Crit. Care 15 (2004) 61–68.
[3] T. Peters Jr., All about Albumin: Biochemistry, Genetics, and Medical Applications, 1st ed., Academic press, US, 1995.
[4] F. Kratz, B. Elsadek, Clinical impact of serum proteins on drug delivery, J. Control. Release 161 (2012) 429–445.
[5] D. Zhao, X. Zhao, Y. Zu, J. Li, Y. Zhang, R. Jiang, Z. Zhang, Preparation, characterization, and in vitro targeted delivery of folate-decorated paclitaxel-loaded bovine serum albumin nanoparticles, Int. J. Nanomed. 5 (2012) 669–677.
[6] G. Gong, Q. Pan, K. Wang, R. Wu, Y. Sun, Y. Lu, Curcumin-incorporated albumin nanoparticles and its tumor image, Nanotechnology 26 (2015) 045603.
[7] B. Subia, S.C. Kundu, Drug loading and release on tumor cells using silk fibroin-albumin nanoparticles as carriers, Nanotechnology 24 (2013) 035103.
[8] X.Y. Teng, Z.Z. Guan, Z.W. Yao, D.G. Liu, N.N. Zhou, H.Y. Luo, M. Hawkins, P. Soon-Shiong, M. Ergul, M. Ergul, Y. Tutar, Important anti-cancer applications of protein based nanoparticles, Curr. Proteom. 10 (2013) 334–340.
[9] J.Y. Jun, H.H. Nguyen, S.Y.R. Paik, H.S. Chun, S.Ko Kang Byeong-Cheol, Preparation of size-controlled bovine serum albumin (BSA) nanoparticles by a modified desolvation method, Food Chem. 127 (2011) 1892–1898.
[10] N.P. Desai, P. Soon-Shiong, Methods and compositions useful for administration of chemotherapeutic agents, (1997) US patent 6.096.33.
[11] N. Wiedenmann, D. Valdecanas, N. Hunter, S. Hyde, T.A. Buchholz, L. Milas, K.A. Mason, 130-nm Albumin-bound Paclitaxel enhances tumor radiocurability and therapeutic gain, Clin. Cancer Res. 13 (2007) 1868–1874.
[12] S.Y.R. Paik, H.H. Nguyen, J. Ryu, J.H. Che, T.S. Kang, J.K. Lee, C.W. Song, S. Ko, Robust size control of bovine serum albumin (BSA) nanoparticles by intermittent addition of a desolvating agent and the particle formation mechanism, Food. Chem. 141 (2013) 695–701.
[13] K. Weber, C. Coester, J. Kreuter, K. Langer, Desolvation process and surface characterisation of protein nanoparticles, Int. J. Pharm. 194 (2000) 91–102.
[14] S.L. Soto Espinoza, M.V. Sánchez, V. Risso, E.E. Smolko, M. Grasselli, Radiation synthesis of seroalbumin nanoparticles, Radiat. Phys. Chem. 81 (2012) 1417–1421.
[15] G.H.C. Varca, C.C. Ferraz, P.S. Lopes, M.B. Mathor, M. Grasselli, A.B. Lugao, Radio-synthesized protein-based nanoparticles for biomedical purposes, Radiat. Phys. Chem. 94 (2014) 181–185.
[16] G.H.C. Varca, G.G. Perossi, M. Grasselli, A.B. Lugao, Radiation synthesized protein-based nanoparticles: A technique overview, Radiat. Phys. Chem. 105 (2014) 48–52.
[17] ISO/ASTM516-13 Standard Practice for Use of the Alanine-EPR Dosimetry System.
[18] U.K. Laemmli, Cleavage of structural proteins during assembly of the head of bacteriophage T4, Nature 227 (1970) 680–685.
[19] T. DiMarco, C. Giulivi, Current analytical method for the detection of dityrosine, a biomarker of oxidative stress in biological systems, Mass Spectrom. Rev. 26 (2006) 108–120.
[20] L. Willard, A. Ranjan, H. Zhang, H. Monzavi, R.F. Boyko, B.D. Sykes, VADAR: web server for quantitative evaluation of protein structure quality, Nucleic Acids Res. 31 (2003) 3316–3319.
[21] A. Shrake, J.A. Rupley, Environment and exposure to solvent of protein atoms. Lysozyme and insulin, J. Mol. Biol. 79 (1973) 351–371.
[22] Jmol an open-source Java viewer for chemical structures in 3D. http://www.jmol.org/.
[23] J.A. Gerrard, Protein–protein crosslinking in food: methods consequences, applications, Trends Food Sci. Tech. 13 (2002) 391–399.
[24] C. Sabliov, H. Chen, R. Yada, Nanotechnology and Functional Foods: Effective delivery of bioactive ingredients, 1st ed., John Wiley & Sons Ltd., 2015, pp. 282.
[25] H. Yoshikawa, A. Hirano, T. Arakawa, K. Shiraki, Effects of alcohol on the solubility and structure of native and disulfide-modified bovine serum albumin, Int. J. Biol. Macromol. 50 (2012) 1286–1291.
[26] S. Kadlubowski, Radiation-induced synthesis of nanogels based on poly(*N*-vinyl-2-pyrrolidone)—a review, Radiat. Phys. Chem. 102 (2014) 29–39.
[27] S. Adhikari, C. Gopinathan, Oxidation reactions of bovine serum albumin-bilirubin complex. A pulse radiolysis study, Int. J. Radiat. Biol. 69 (1995) 89–98.
[28] M.H. Gaber, Effect of γ-irradiation on the molecular properties of bovine serum albumin, J. Biosci. Bioeng. 100 (2005) 203–206.
[29] C. Giulivi, N.J. Traaseth, K.J. Davies, Tyrosine oxidation products: analysis and biological relevance, Amino Acids 25 (2003) 227–232.
[30] P. Ulanski, S. Kadlubowski, J.M. Rosiak, Synthesis of poly(acrylic acid) nanogels by preparative pulse radiolysis, Radiat. Phys. Chem. 63 (2002) 533–537.
[31] R. Gossmann, E. Fahrländer, M. Hummel, D. Mulac, J. Brockmeyer, K. Langer, Comparative examination of adsorption of serum proteins on HSA- and PLGA-based nanoparticles using SDS–PAGE and LC–MS, Eur. J. Pharm. Biopharm. 93 (2015) 80–87.
[32] W. Wang, Y. Huang, S. Zhao, T. Shaoa, Y. Cheng, Human serum albumin (HSA) nanoparticles stabilized with intermolecular disulfide bond, Chem. Commun. 49 (2013) 2234–2236.
[33] B.J. Endrizzi, G. Huang, P.F. Kiser, R.J. Stewart, Specific covalent immobilization of proteins through dityrosine cross-links, Langmuir 22 (2006) 11305–11310.
[34] C. Houée-Levin, K. Bobrowski, The use of the methods of radiolysis to explore the mechanisms of free radical modifications in proteins, J. Proteom. 92 (2013) 51–62.
[35] C. Houée-Lévin, K. Bobrowski, L. Horakova, B. Karademir, C. Schöneich, M.J. Davies, C.M. Spickett, Exploring oxidative modifications of tyrosine: An update on mechanisms of formation, advances in analysis and biological consequences, Free Radic. Res. 49 (2015) 347–373.
[36] G.E. Adams, J.W. Boag, J. Currant, B.D. Michael, in: M. Ebert, J.P. Keene, A.J. Swallow, J.H. Baxendale (Eds.), Pulse Radiolysis, Academic Press, New York, 1965, pp. 131–143.
[37] G.V. Buxton, C.L. Greenstock, W.P. Helman, A.B. Ross, Critical review of rate constants for reactions of hydrated electrons, hydrogen atoms and hydroxyl radicals ($^{\bullet}OH/^{\bullet}O^{-}$) in aqueous solution, J. Phys. Chem. Ref. Data 17 (1988) 513–886.
[38] I. Rombouts, B. Lagrain, K.A. Scherf, P. Koehler, J.A. Delcour, Formation and reshuffling of disulfide bonds in bovine serum albumin demonstrated using tandem mass spectrometry with collision-induced and electron-transfer dissociation, Sci. Rep. 5 (2015) 12210.
[39] S.K. Kapoor, C. Gopinathan, Evidence for possible positive hole transport in the biological protein bovine serum albumin, J. Radioanal. Nucl. Chem. 171 (1993) 443–450.
[40] A. Plonka, R. Krasiukianis, J. Mayer, A. Zgirski, M. Hilewicz-Grabska, Pulse-radiolysis studies on reactivity of BSA and BSA-Cu(II) complexes, Radiat. Phys. Chem. 38 (1991) 445–447.
[41] A. Bujkacz, G. Bujacz, Structures of bovine, equine and leporine serum albumin, Acta Crystallogr. Sect. D 68 (2012) 1278–1289.
[42] O. Mozziconacci, J. Mirkowski, F. Rusconi, G. Kciuk, P.B. Wisniowski, K. Bobrowski, C. Houée-Levin, Methionine residue acts as a prooxidant in the $^{\bullet}OH$-induced oxidation of enkephalins, J. Phys. Chem. B 116 (2012) 12460–12472.